Performance Evaluation of an Enhanced Bus Differential Protection Relay

Nuwan Perera, K Ponram
ERLPhase Power Technologies Ltd.
Winnipeg, MB, Canada

Abstract—**The busbar protection relays typically implements low impedance percentage differential principle using dual slope characteristics. These relays may sometimes misoperate in response to the CT saturation during close-in external faults, and the subsidence current present after clearing external faults. A primary reason for such misoperations is the fact that the traditional percentage differential principle relies exclusively on current magnitudes rather than directionality for tripping decisions. This paper evaluates the performance of an enhanced bus differential relay which uses different principles that distinguish between external and internal faults so as to enhance the security of differential protection. Extensive testing has been carried out to evaluate the effectiveness of the new principles in enhancing the security for external faults.**

***Index Terms*—differential protection, busbar protection, CT saturation, phase angle, faults**

I. Introduction

Security, reliability and fast response (often within 1 cycle) are vital criteria in busbar and transformer protection. In the past, busbars and transformers were protected using conventional electro-mechanical relays that operated on the principle of current unbalance when there is a fault inside the protected zone [1-4]. Although microprocessor based differential relays are currently being used, most of these relays still operate based on a low impedance percentage differential principle adopted from the conventional electromechanical relays.

A typical dual slope differential characteristic of a conventional relay is shown in Fig. 1. Here, **Io** and **Ir** are called the operating current and the restraint current respectively. The operating current is defined as the magnitude of the sum of vector currents whereas, the restraint current is defined as the sum of individual current magnitudes divided by two. This dual slope characteristic allows the users to define a minimum pickup level, $\mathbf{Io_{min}}$ and two slopes **S1** and **S2**. The minimum pickup level allows typical bus loading. The slopes, **S1** and **S2** allows for current transformer (CT) errors during normal load conditions and external fault conditions near the bus.

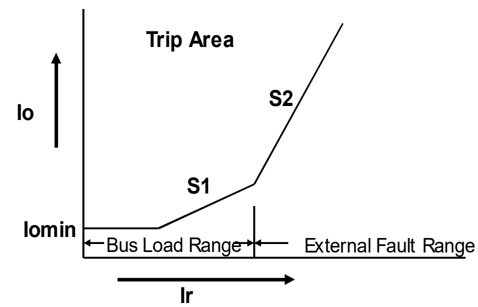

Fig.1: Dual slope characteristic of traditional relay

Although the above dual slope characteristic provides some security against CT errors, it is not adequate for all practical scenarios. Two common failures reported with conventional dual slope characteristics are due to CT saturation which occurs during close-in external faults and the subsidence currents present after clearing external faults.

This paper investigates the performance of an enhanced differential relay implemented to overcome aforementioned protection issues using a real time digital simulator. Rest of the paper is organized as follows. Section II presents principles of internal and external fault identification methods specific to the protection scheme under evaluation. The enhanced differential protection scheme is presented in Section III. The test results are presented in Section IV. Finally, the conclusions are given in Section V.

II. Principles of Internal and External Fault Identification

A. Phase Angle Comparison Method

The preservation of current phase angle always takes place even if CT saturation or dc offset conditions occur to the input ac currents. As a result, if the phase angle of the current waveforms is compared with the phase angle of each of the input bus currents, a decision can be made whether a fault is external or internal to the differential protected zone irrespective of the waveform distortions due to the errors in CTs. Comparing phase currents in near real time, a comparison can be made between currents that are entering the bus and those currents that are leaving the bus. This is intuitively true since Kirchoff's law also applies to phase angles as well as to current magnitudes.

However, the key challenge in this method is estimation of phase angles between all current phase angles rapidly in real-time. In this paper, a technique that utilizes the dot product was used to determine the differences in phase angles.

If **A** and **B** are vectors, the dot product is defined as,

$$\boldsymbol{A} * \boldsymbol{B} = AB\cos\,\theta \tag{1}$$

where, A and B are scalars θ is the angle between the vectors.

The vectors $\boldsymbol{A}$ and $\boldsymbol{B}$ can also be represented by the following equations:

$$\boldsymbol{A} = a_1 + ja_2 \tag{2}$$

$$\boldsymbol{B} = b_1 + jb_2 \tag{3}$$

Therefore, their dot product becomes:

$$\boldsymbol{A} * \boldsymbol{B} = a_1b_1 + a_2b_2 \tag{4}$$

In this paper, the dot product $\boldsymbol{A} * \boldsymbol{B}$ calculated using (4) was used. The calculation of dot product using this method has the advantage of avoiding cosine function estimations. This significantly reduces the amount of computations involved compared to the conventional approach. More details about this implementation can be found in [5].

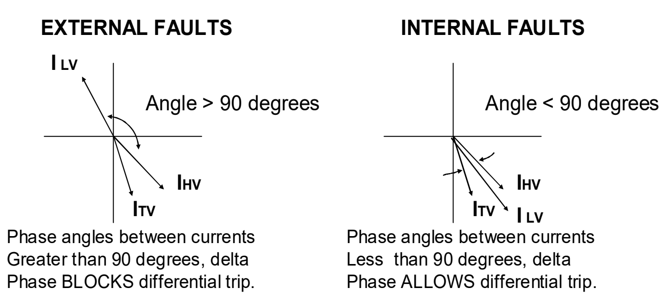

Fig.2: Current phases during internal faults and external faults

Comparison of phase angles of currents at every sample point allows the slope characteristic algorithm to be supervised by the phase angle function. In this implementation, the phase angle difference for discrimination of fault/no fault conditions is set to 90 degrees, so if all current phasors are within 90 degrees or less (from each other), tripping by the slope characteristic is allowed. If the measured current phasors are within an angle greater than 90 degrees, the event is recognized as an external fault and tripping is blocked. If only one current input is present, no phase angle comparisons can be made. In such situations, tripping is permitted only if the slope characteristic operates. The logic used in phase angle function is illustrated in Fig. 2.

B. Differential Rate of Change Method

In practical applications, not all the elements connected to bus will have active sources behind them. As a result, during an internal bus fault, especially with fault impedance, load flow may continue to flow on these passive elements and may cause the phase angles function to block the relay from tripping for the internal fault even though the slope characteristic may detect the fault. In order to overcome this issue, an additional function was integrated into the differential relay operation. As it can be seen from Fig.3, during faults **Io** and **Ir** quantities will change independently of the type of the fault. It can be further observed that for an internal bus fault, the rate of change of **Io** (**dIo / dt**) is greater than the rate of change of **Ir** (**dIr / dt**), whereas for external faults, **dIr / dt** is greater than **dIo / dt**. Thus, the "Rate-of-Change-of-Differential" (ROCOD) can be used as a supervisory function for slope characteristics when phase angle comparison function is involved. More details of this concept can be found in [6].

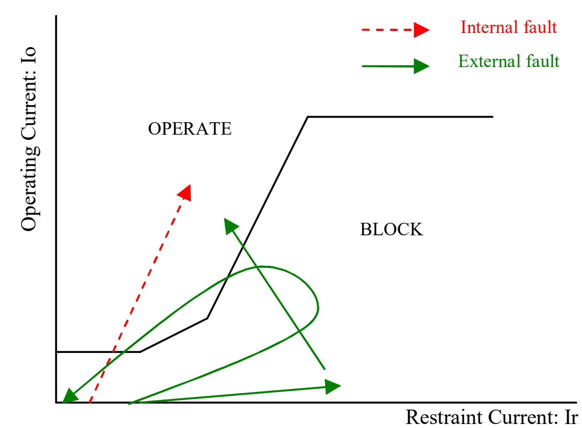

Fig.3: Variation of Io and Ir during internal and external faults

III. ENHANCED DIFFERENTIAL PROTECTION SCHEME

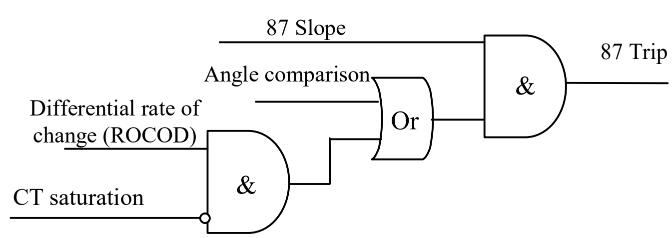

Fig.4: Basic logic for enhanced differential protection scheme

In order to enhance the security of the conventional differential protection, a new protection algorithm was implemented combining concepts described above in Section II. The basic logic for the enhanced bus differential protection scheme that combines the slope characteristic, the phase angle function and the ROCOD function is shown in Fig.4.

The individual functions in the proposed bus differential protection scheme (shown in Fig.4) operate as follows:

- SLOPE function goes to logic "1" output when **Io** exceeds the slope characteristic.
- Phase Angle function goes to logic "1" for an internal fault.
- The ROCOD (rate of change of **Io** and **Ir**) goes to logic "1" for an internal fault. Further, the function is blocked if any CT saturation is detected

The algorithm used for detection of CT saturation was implemented based on the method proposed in [7].

A. Operation during Internal Faults

The slope characteristic will operate during a fault internal to the bus. The ROCOD logic and possibly the phase angle function may operate. When this happens, the slope function will be allowed to trip. In some cases where passive element loads are present, the ROCOD function will operate before the phase angle logic. In some other cases where bus elements have sources behind them, both the ROCOD and the phase angle will operate. This will ensure fast and secure operation during internal fault conditions.

B. Operation during External Faults

During the faults external to the bus, the slope characteristic should not pickup unless current waveform distortion occurs. If this happens, ROCOD output will be zero and the phase angle output will also be zero. This will result in a NO TRIP condition. This arrangement ensures correct operation during CT saturations resulting from close-in external faults and the subsidence currents present after clearing the external faults.

In order to verify the operation of modified bus differential protection algorithm, testing was carried out using real time data generated using an electromagnetic transient simulation program and details are given in the following section.

IV. Testing

A. Test Setup

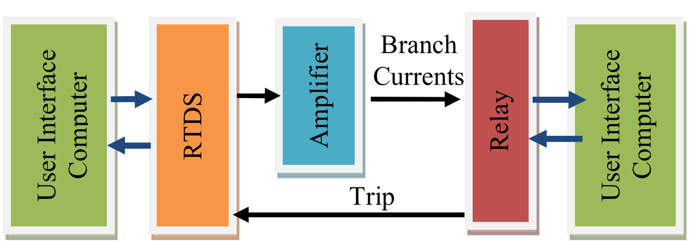

Fig.5: Test setup

The real-time waveforms required to test the relay were generated from a test system simulated in real time digital simulator (RTDS). The schematic diagram of closed-loop test setup used for relay testing is shown in Fig.5. The analog waveforms generated from RTDS were sent to the relay via an amplification circuit. The trip signal generated by the relay was fed back into the RTDS. The user interface for RTDS and relay was provided by using two personal computers.

B. Test System

The network configuration of 230 kV, transmission system simulated in RTDS is shown in Fig.6. The transmission lines were simulated using frequency dependent transmission line models. The transformers were modeled including the saturation effects. The three-phase current signals corresponding to each of the line connected to the protected bus ($\mathbf{I_1}$, $\mathbf{I_2}$, $\mathbf{I_3}$ and $\mathbf{I_4}$) were monitored. The CTs were also modeled to include the effects of saturation. Faults were simulated at different locations of the network with different fault impendences. The results obtained using RTDS are presented below.

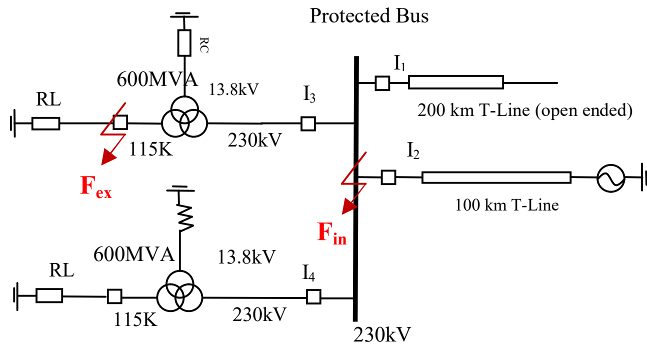

Fig.6: Network configuration

C. Test Results

Fig. 7 illustrates a case of an external fault ($\mathbf{F_{ex}}$) with slow CT saturation resulted in picking up the slope characteristics. It can be seen that the currents are out of phase, and the third input ($\mathbf{I_3}$) is approximately 180 degrees away from the other two ($\mathbf{I_2}$ and $\mathbf{I_4}$). The phase angle function output would therefore be zero, blocking any tripping. In addition, the values of the differential **Io** and **Ir** are also shown. If the derivative of these quantities is taken, a positive output would occur when the **Io** and **Ir** values are changing. It can be seen that the **dIr/dt** positive value exceeds the **dIo/dt** positive value, indicating an external fault. As a result, the output of ROCOD will be zero, also blocking any possible tripping by the slope characteristic.

Fig. 8 shows an example of a high impedance (200 ohms) phase A-G internal fault ($\mathbf{F_{in}}$). As there is only one active current contribution, the phase angle function would logically go to a "0" value, blocking the operation. However, the ROCOD function would go to logic "1" since the positive derivative value of **dIo/dt** exceeds **dIr/dt**. This enables the protection logic to identify the internal fault correctly. As it can be seen from Fig.8, the relay was able to identify the internal fault within less than a half cycle time period. It should be noted that the algorithm is capable of discarding any high frequency oscillations observed in open ended transmission lines during the faults.

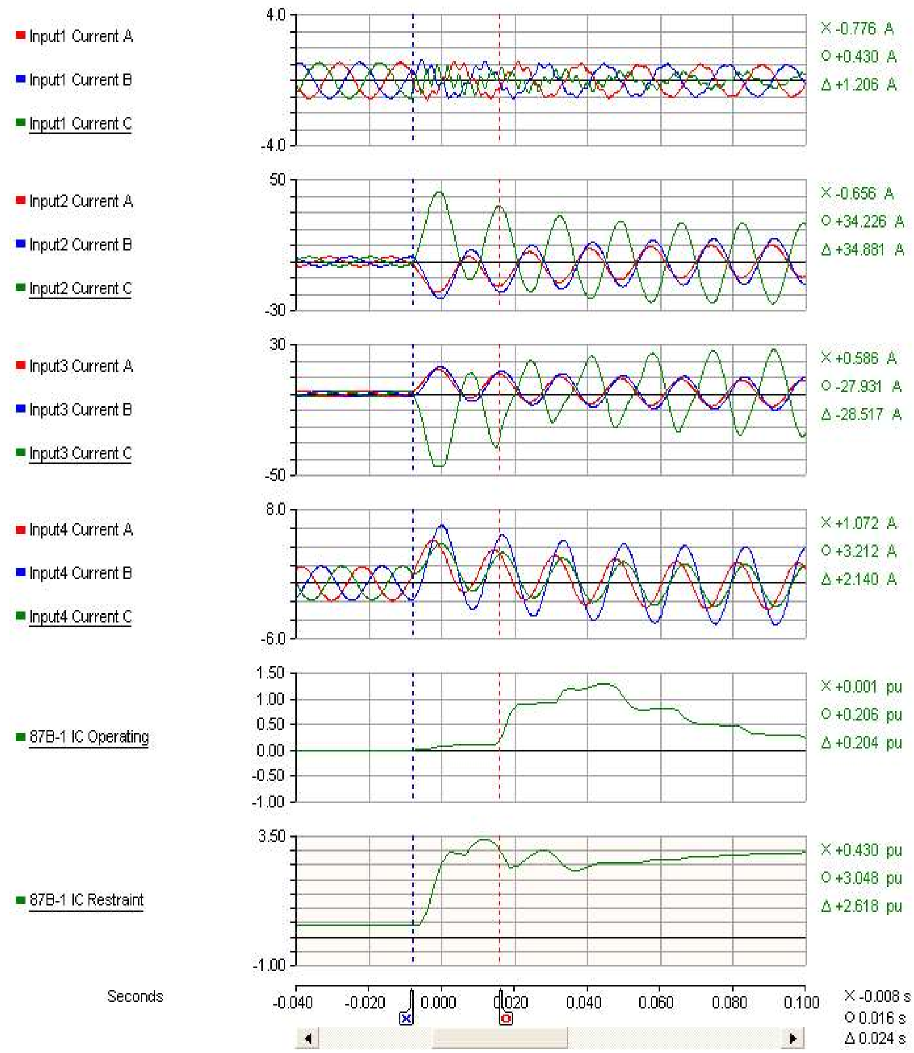

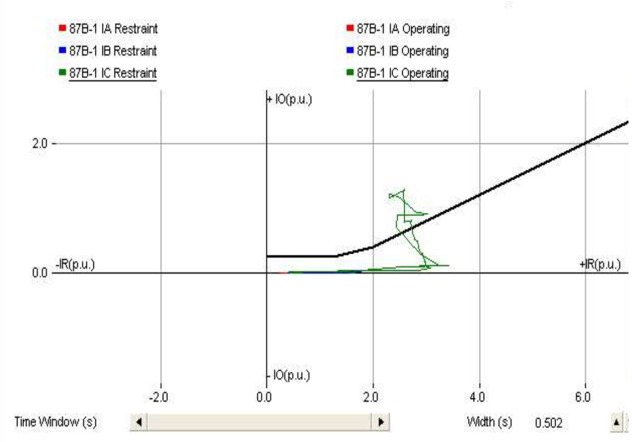

Fig.7: Three-phase current signals, restraint current, operating current and slope characteristics for Phase C-G external fault with CT saturation

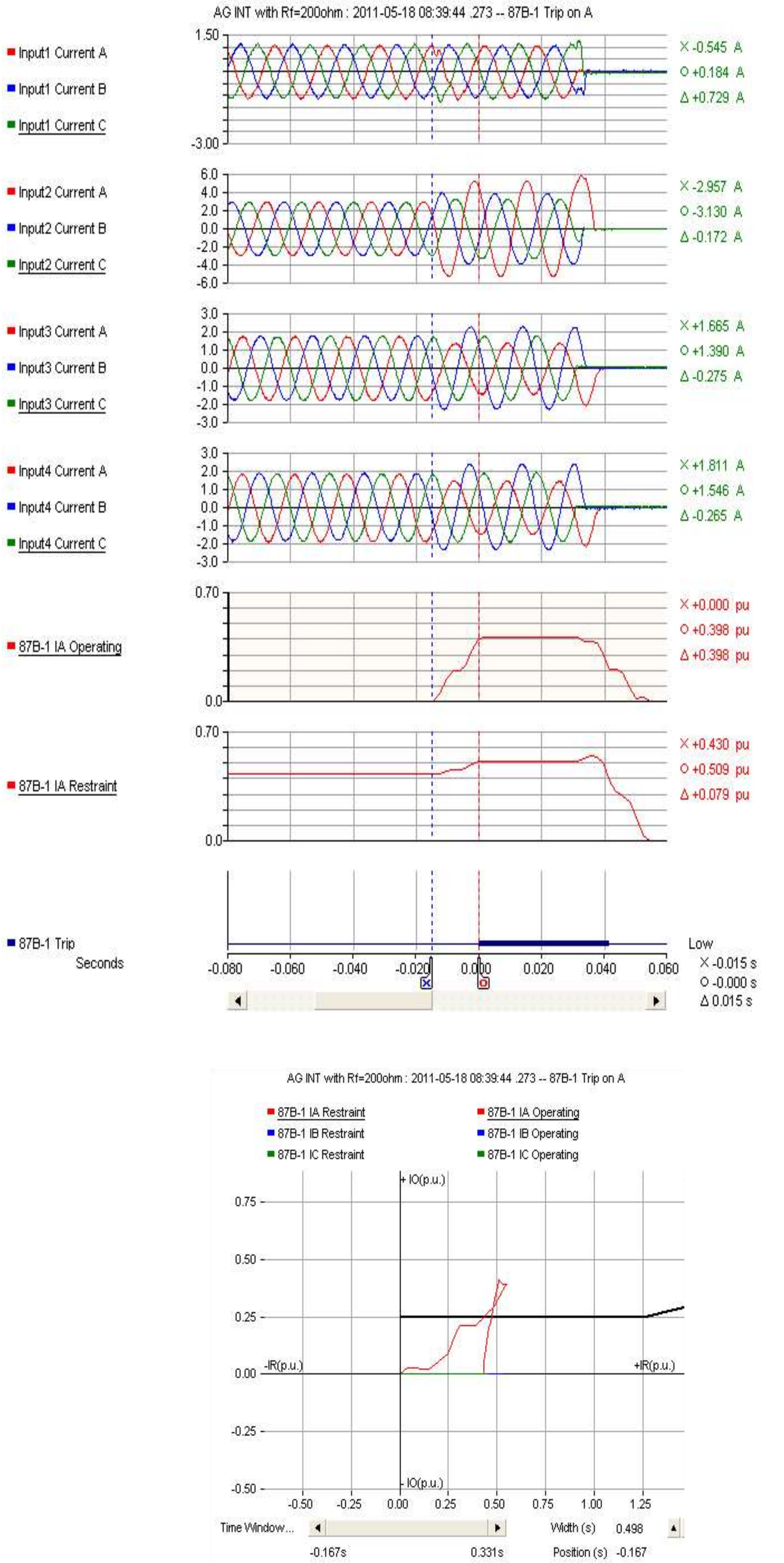

Fig.8: Three-phase current signals, restraint current, operating current, trip signal and slope characteristics for Phase A-G high impedance internal fault

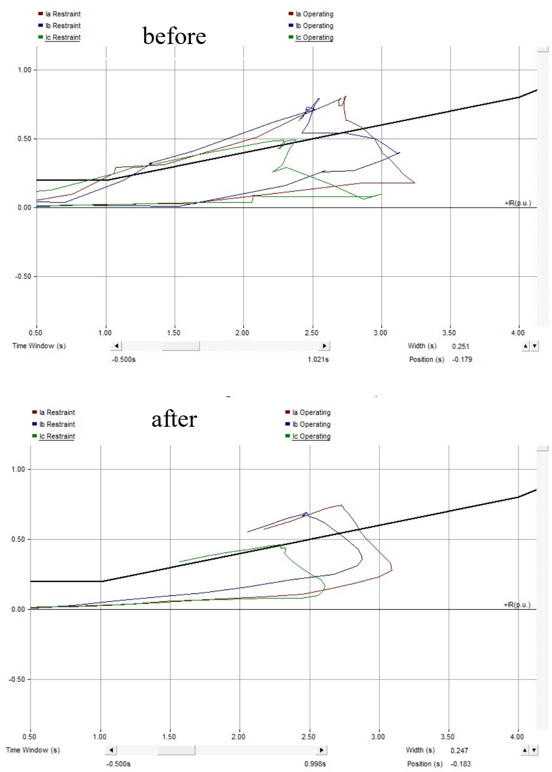

Fig.9: Effect of Advanced Filtering

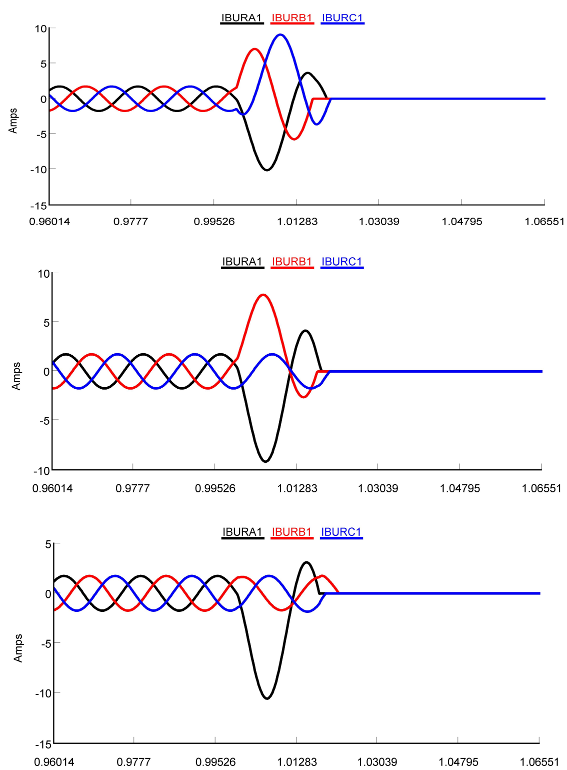

Fig.10: Operating time

Fig.9 shows the impact of the advanced filtering methods used by the relay. As it can be observed from Fig.9, application of filter helps to eliminate the noise generated due to high frequency transients. Speed of operation was tested for different types of faults. Fig.10 shows the waveforms captured by the RTDS simulator during the closed loop testing, showing one cycle fault clearing including the relay output contact operations.

V. Conclusions

Applicability of an enhanced bus protection scheme was investigated using a transmission network simulated in a real time digital simulator. Performance of the scheme was tested using different types of events simulated under different practical scenarios such as fast CT saturation, slow CT saturation, high fault impedances, dc offset, etc.. The results obtained from this study showed the capabilities of the selected relay in detecting internal and external faults accurately even if the input current waveforms are distorted or offset.

VI. References

[1] J. G. Adrichak and J. Cardenas, “Bus differential protection”, *22nd WPRC Conference*, Spokane, October 1995, pp. 1-11.

[2] C. R. Mason, “The art and science of protective relaying”, *John Wiley & Sons*, New York, 1956.

[3] W. Rebizant, T. Hayder and L. Schiel, “Prediction of CT saturation period for differential relay adaptation purposes”, *International Conference on Advanced Power System Automation and Protection*, Korea, 2004, pp. 1-6.

[4] C. Fernandez, “An Impedance based CT saturation detection algorithm for Bus-Bar differential Protection”, *IEEE Trans. on Power Delivery*, vol 16, no. 4, pp. 468-472, Oct. 2001.

[5] K. Narendra and D. Fedirchuk, “Secured busbar differential protection using a computationally efficient dot product technique, *Power System Protection and Automation*, India, 2010.

[6] K. Narendra, D. Fedirchuk and N. Zhang, “Differential rate of change method for busbar protection”, US Patent. Pending (Submitted-2010)

[7] D. Fedirchuk, G. Li, Z. Zhang, D.S. Ouellette, “Electrical bus protection method and apparatus”, US Patent - 7,199,991 B2, Issued April 2007.